JOURNAL OF Applied Polymer SCIENCE

Characterization and Biocompatibility of Chestnut Shell Fiber-Based Composites with Polyester

Chin-San Wu,[1] Yi-Chiang Hsu,[2,3] Hsin-Tzu Liao,[1] Fu-San Yen,[4] Chen-Yu Wang,[4] Chia-Tsc Hsu[1]

[1]Department of Chemical and Biochemical Engineering, Kao Yuan University, Kaohsiung 82101, Taiwan, Republic of China

[2]Graduate Institute of Medical Science, College of Health Sciences, Chang Jung Christian University, Tainan 71101, Taiwan, Republic of China

[3]Innovative Research Center of Medicine, College of Health Sciences, Chang Jung Christian University, Tainan 71101, Taiwan, Republic of China

[4]Department of Chemical and Material Engineering, National Kaohsiung University of Applied Sciences, Kaohsiung 807, Taiwan, Republic of China

Correspondence to: C.-S. Wu (E-mail: t50008@cc.kyu.edu.tw)

ABSTRACT: The structural, mechanical, biocompatibility, and biodegradability properties of composite materials formed of poly(butylene succinate) (PBS) and natural fiber (chestnut shell fiber; CSF) were evaluated. Maleic anhydride-grafted poly(butylene succinate) (PBS-*g*-MA) and treated (crosslinked) CSF (TCSF) were used to improve the mechanical properties of PBS/CSF composites. The results show that PBS-*g*-MA/TCSF composites have superior mechanical properties compared with both pure PBS and PBS/CSF composites, which is attributed to better compatibility between the polymer and TCSF. Normal human foreskin fibroblasts (FBs) were seeded onto these two series of composites to characterize the biocompatibility. FB proliferation, collagen production, and cytotoxicity assays on the PBS/CSF series of composites exhibited superior results compared with those on the PBS-*g*-MA/TCSF composites. PBS-*g*-MA/TCSF was found to be more water resistant than PBS/CSF, and the weight loss of both the composites buried in soil compost indicated that both were biodegradable, especially at high levels of CSF substitution. © 2014 Wiley Periodicals, Inc. J. Appl. Polym. Sci. **2014**, *131*, 40730.

KEYWORDS: biocompatibility; biodegradable; blends; fibers; polyesters

Received 17 December 2013; accepted 18 March 2014

DOI: 10.1002/app.40730

INTRODUCTION

Biomedical materials are natural or synthesized materials that (directly or indirectly) contact with human tissue, body fluids, or blood and can be embedded or integrated into living systems to replace or repair parts of a living system or to contact the living body directly to perform a vital function.[1–3] Therefore, biomedical materials should be biocompatible, bioabsorbable, and/or facilitate tissue regeneration.[4,5] Biomedical materials can be classified into metals, ceramics, and polymers[6–8]; polymers are the most common materials, because they are highly biocompatible with human tissue and blood, as well as nontoxic, workable, and resolvable.[9–11]

Biodegradable polymers are extensively used in biomedical applications. Common biodegradable polymers include polylactic acid, polyhydroxyalkanoate (PHA), poly(butylene succinate);(PBS), and polycaprolactone.[12–14] PBS is derived from succinic acid and butanediol via condensation polymerization, can be easily formed into different shapes, is biocompatible and bioabsorbable,[15–17] and can be decomposed and metabolized by multiple microbial enzymes. It is a fully biodegradable polymer, which can be resolved into carbon dioxide and water. However, it is relatively expensive, and so mixing it with plant fibers to reduce cost may be desirable; furthermore, the mechanical properties of these polymers may be improved by the formation of the composite material.

Plant fibers may be obtained by processing and recycling agricultural waste. Suitable fibers include chestnut shell fiber (CSF), bamboo fiber, rice straw, and husk. They are inexpensive, abundant resources, biodegradable, nontoxic, and can be reused extensively.[18–20]

The structure of chestnut shell is mainly composed of fibers. After grinding treatment, the chestnut shell can be used as a covering material to blend with biodegradable polymers to prepare the green composites.[21] Tannins in the CSF extraction and chemical composition may restrain proteins, promote tissue regeneration, promote wound healing, and inhibit cancers. For these reasons, CSF is a preferred filler-reinforcement material. However, in the processing of plant fibers and biodegradable

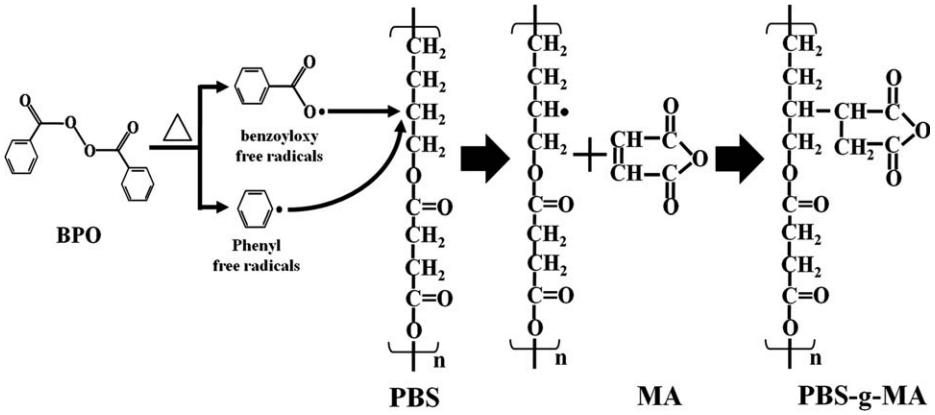

Scheme 1. he mechanism grafting structure reaction of MA onto PBS.

polymers, the mechanical properties are typically degraded following the addition of plant fibers, due to the weak binding between the polymer and the plant fiber. To enhance the binding between the polymer and plant fiber, a polar group may be grafted onto the biodegradable polymer side chain to bond to the —OH groups of plant fiber, improving the mechanical strength of the composite material.

Here, we report the use of a crosslinking agent with treated CSF (TCSF) to prepare PBS-based composites. We studied the mechanical properties of TCSF-containing composites formed with pure PBS and maleic anhydride-grafted PBSPBS-*g*-MA. The structural changes in the composites that were induced by the MA moiety were studied using Fourier transform infrared (FTIR) spectroscopy and ^{13}C nuclear magnetic resonance (NMR) spectroscopy. The biocompatibility of composites was characterized using cell surface adhesion, soluble collagen, and cytotoxicity assays.

EXPERIMENTAL

Materials

PBS (GS Pla®FZ91 P) was supplied by Mitsubishi Chemical Performance Polymers (Japan), with a weight-average molecular weight (M_w) of 4.72×10^4, a number-average molecular weight (M_n) of 3.68×10^4, a polydispersity index of 1.28, aspect ratio 4–10; MA, benzoyl peroxide (BPO), propidium iodide (PI), phosphate-buffered saline, dimethyl sulfoxide (DMSO), and 3-(4,5-dimethylthiazol-2-yl)-2,5-diphenyltetrazoleliumbromide (MTT) were purchased from Sigma-Aldrich Chemical (St. Louis, MO); fetal bovine serum (FBS) and Dulbecco's modified Eagle's medium (DMEM) were purchased from Gibco-BRL (Gaithersburg, MD); binding buffer and Annexin V-FITC apoptosis detection kits were obtained from Becton Dickinson (Franklin Lakes). All buffers and other reagents were the highest purity grade that was commercially available. CSF is mainly composed of cellulose, hemicellulose, lignin, other constituents of polyphenol compounds, polyphenol oxidase, peroxidise, metal ions (Fe, K, Na, ...), and so forth.

PBS-*g*-MA Copolymer

The grafting reaction of MA onto PBS is illustrated in Scheme 1. In preliminary testing using dichloromethane as a solvent, a mixture of MA and BPO was added in four equal portions at 2-min intervals to the PBS to allow grafting to take place. The reactions were performed in a nitrogen (N_2) atmosphere at $50 \pm 2°C$. Preliminary results showed that reaction equilibrium was attained in less than 12 h. Thus, reactions were allowed to progress for 12 h while stirring at 60 rpm. The product (4 g) was dissolved in 200 mL of refluxing dichloromethane at $50 \pm 2°C$, and the solution was filtered through several layers of cheesecloth. The dichloromethane-insoluble product that remained on the cheesecloth was washed using acetone to remove the unreacted MA and was then dried in a vacuum oven at 80°C for 24 h. The dichloromethane-soluble product in the filtrate was extracted using 600 mL of cold acetone; this extraction was repeated five times. The percentage of grafted polymer was determined using a titration method,[22] which showed that the grafting percentage was approximately 0.98 wt %. BPO and MA loadings were maintained at 0.3 wt % and 10 wt %, respectively.

Processing of CSF and TCSF

Scheme 2 shows an overview of the processing of the CSF samples, which consisted of a mixture of fine blackish brown fragments up to 2 cm long. The fragments were processed as follows. First, the crude CSF was dried at 50–60°C under vacuum for 2 days. Then the product was grounded in a high-speed rotary grinder (Yowlin Industrial, Taiwan) six times for 10 min each time and was vacuum dried at 50–60°C for 2 days. The crushed CSF was then passed through a 200-mesh sieve, and the resulting CSF, with dimensions of approximately 100–300 μm, was purified by immersing 60 g of the CSF in 1000 mL of distiled water for 2 days to remove any water-soluble components. The CSF samples were air-dried for 2 days at 50–60°C and then vacuum dried at 105°C for 8 h, resulting in a moisture content of $5.0 \pm 0.2\%$ by weight.

A mixture of crosslinking agents was prepared by dissolving stoichiometric amounts of tetraethyl orthosilicate (TEOS), H_2O, and lactic acid catalyst in tetrahydrofuran, stirring the solution at room temperature for 1 h, and then allowing the solution to stand for 2 days. The molar ratios used were as follows: lactic acid/TEOS = 0.01 and H_2O/TEOS = 2.2. The CSF and crosslinking agents were mixed at room temperature for 1 h at a rotor speed of 50 rpm. Samples were prepared with mass ratios of

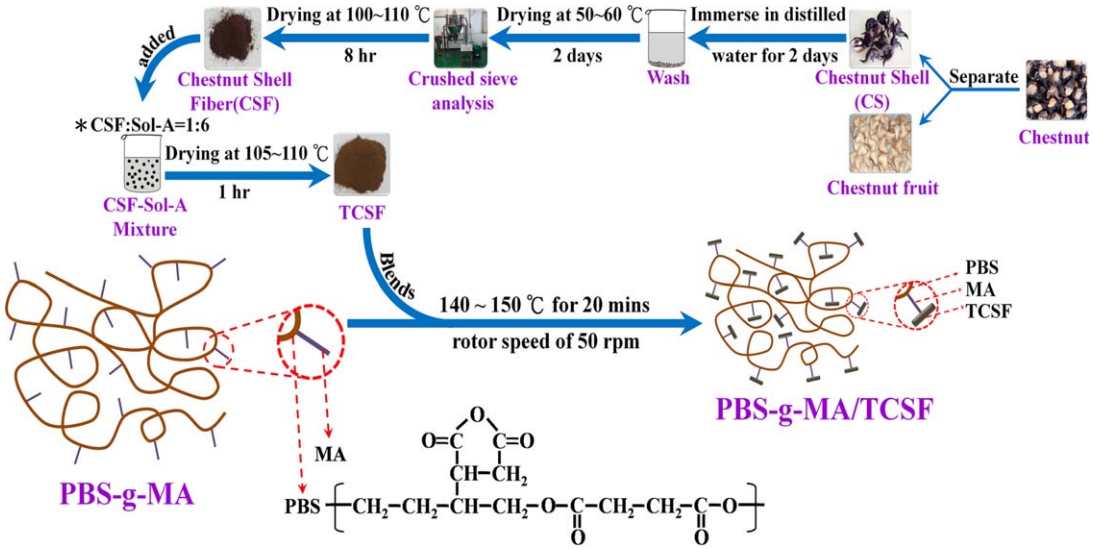

Scheme 2. The preparation of the crosslinked CSF and the composite materials. [Color figure can be viewed in the online issue, which is available at wileyonlinelibrary.com.]

CSF to crosslinking agents of 1 : 6. The final product was dried under vacuum at 105–110°C for 24 h.

Composite Preparation

The prepared CSF samples were washed with acetone and dried in an oven at 105°C for 24 h. Composites were prepared in a Plastograph 200-Nm Mixer W50EHT (Brabender, Dayton, OH) with a blade rotor (Brabender). They were mixed at 140–150°C for 20 min at a rotor speed of 50 rpm. Samples were prepared with mass ratios of CSF or TCSF to PBS or to PBA-*g*-MA of 5 : 95, 10 : 90, 15 : 85, and 20 : 80. Residual MA in the PBS-*g*-MA reaction mixture was removed via acetone extraction prior to the preparation of the PBS-*g*-MA/TCSF composite. After mixing, the composites were pressed into thin plates with a 150°C hot press and placed in a dryer for cooling. These thin plates were cut into standard sample dimensions for further characterization.

Characterization

NMR and FTIR Analyses. Solid-state ^{13}C NMR and ^{29}Si NMR spectra were acquired using an AMX-400 NMR spectrometer at 100 MHz under cross-polarization while spinning at the magic angle. Power decoupling conditions were set with a 90° pulse and a 4-s cycle time. Contact time 2.0 ms were used. Samples were loaded into 4-mm fused zirconia tubes and sealed with Kel-FTM caps. Spectra were obtained at a spinning rate of about 4700 Hz. Infrared spectra of the samples were obtained using an FTS-7PC FTIR spectrophotometer (Bio-Rad, Hercules, CA). The spectra were the results at 2 cm^{-1} resolutions between 400 and 4000 cm^{-1} with collection times of approximately 1 min.

Mechanical Testing. A mechanical tester (model LR5K; Lloyd Instruments, Bognor Regis, West Sussex, UK) was used to measure the tensile strength at failure, in accordance with ASTM Standard D638. Test samples were prepared using a hydraulic press at 150°C and conditioned at a relative humidity of 50 ± 5% for 24 h prior to taking measurements. Testing was performed at a crosshead speed of 10 mm per minute, and mean values were determined based on five specimens for each measurement.

Composite Morphology. A thin film of each composite was prepared with a hydraulic press and treated in a vacuum oven at 60°C for 24 h to obtain samples with dimensions of 150 × 150 × 1 mm^3. Specimens were cut according to the ASTM D638 specifications. Following failure, a thin section of the fracture plane was removed, coated with gold, and imaged using a scanning electron microscope (SEM; S-1400; Hitachi, Tokyo, Japan) to observe the morphology of the fracture surface.

Biofunctions of Human Foreskin FBs on the PBS Series Composites

Cell and Culture Condition. Normal human foreskin fibroblasts (FBs; HS-68) were obtained from the Bioresource Collection and Research Center in Taiwan. The HS-68 cells were grown in a culture medium containing 90% DMEM with 4 m*M* L-glutamine adjusted with a sodium bicarbonate content of 1.5 g/L and a glucose content of 4.5 g/L, with a 10% mixture of FBS. The cells were cultivated at 37°C in a humidified incubator with a 5% CO_2 atmosphere.

Cell Proliferation Assay. MTT assays were used to evaluate the proliferation of HS-68 cells on the membranes. Sample sheets were placed in 24-well plates and sterilized by exposing them to ultraviolet light for 1 h. Each well plate was embedded with 3–5 × 10^4 cells, which were incubated in an atmosphere of 5% CO_2 at 37°C for 1, 3, and 7 days. At the end of the incubation period, the culture medium in the plates was discarded, and the cells were washed with phosphate-buffered saline. Each well plate was then filled with 100 μL of MTT and placed in a dark environment. The culture was incubated for 5 h to convert the MTT to formazan. The supernatant was then removed and 150 μL of DMSO solution was added to dissolve the formazan. The plates were shaken and stirred to ensure the formation of a uniform solution, and the optical

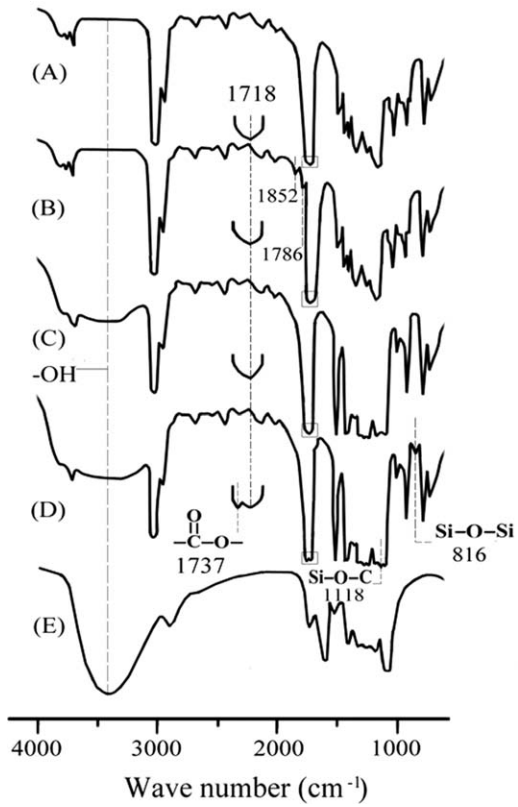

Figure 1. FTIR spectra of (A) PBS, (B) PBS-*g*-MA, (C) PBS/CSF (10 wt %), (D) PBS-*g*-MA/TCSF (10 wt %), and (E) CSF.

density at 540 nm was determined using a Powerwave XS reader (Bio-Tek).

Collagen Quantification Assay. The culture medium fluid (0.1 mL) from the samples and Sircol dye reagent (1 mL) were mixed in a centrifuge tube for 1 h. The mixture was then centrifuged at 12,000 g for 10 min, the supernatant is removed, and the residual liquid on the edge of the centrifuge tube was removed using absorbent paper. Care was taken not to touch the precipitate during the process. An aliquot of 100 μL of 0.1*M* NaOH solution was then added, and the sample was left for 15 min to dissolve the precipitate. After 10 min of stable coloration, 0.2 mL of the resulting liquid was picked up and placed into 96-well plates, and the absorbance at 540 nm was measured.

Evaluation of Cytotoxicity (Apoptosis and Necrosis). Aliquots of 1×10^6 cells per sample were placed into small centrifuge tubes. Cells were spun at 200 g for 5 min, the supernatant was discarded, and pellets were washed with 500 μL of phosphate-buffered saline with 5 μL of Annexin V-FITC and 5 μL of PI labeling solution. The cell suspension was incubated for 15 min at room temperature in the dark. Phosphate-buffered saline (500 μL) was added, and the stained cells were analyzed using flow cytometry (FACSCalibur, BD). Data were analyzed using the WinMDI 2.8 software (BD).

Water Absorption

Samples were prepared for water absorption measurements by cutting them into 50×30 mm^2 strips that were 150 ± 5 μm thick, in accordance with ASTM Standard D570. The samples were dried in a vacuum oven at 50 ± 2°C for 12 h, cooled in a desiccators, and then immediately weighed; this mass is designated W_c. The samples were then immersed in distilled water and maintained at 30 ± 2°C for 14 weeks. During that time, they were removed from the water at 2-week intervals, gently blotted using tissue paper to remove excess water from the surfaces, immediately weighed (this weight is designated W_w), and then returned to the water. Each mass W_w was an average of three measurements. The percent weight increase due to water absorption, W_f, was calculated to the nearest 0.01%, as follows:

$$W_f = \frac{W_w - W_c}{W_c} \times 100 \quad (1)$$

Biodegradation Studies

The biodegradability of the samples was assessed by measuring the weight loss of the composites over time in soil. Samples measuring $50 \times 30 \times 1$ mm^3 were weighed and buried in boxes containing alluvial-type soil obtained from farmland topsoil before planting. The soil was sifted to remove large clumps and plant debris. The procedure for soil burial was as described by Umare et al.[23] The soil was maintained at approximately 35% moisture by weight, and the samples were buried at a depth of 12–15 cm. A control box consisted of samples and no soil. The samples were retrieved after 2 weeks, washed in distilled water, dried in a vacuum oven at 50 ± 2°C for 2 days, and equilibrated in a desiccator for at least 1 day. The samples were then weighed before being returned to the soil.

RESULTS AND DISCUSSION

Characterization of PBS and Its Composites

The FTIR spectrum of unmodified PBS is shown in Figure 1A, and the FTIR spectrum of PBS-*g*-MA is shown in Figure 1B. Characteristic absorption peaks of PBS occur at 3200–3700 cm^{-1} (—OH), 1700–1750 cm^{-1}(—COO—), and 500–1500 cm^{-1} (—C—O),[24]which appeared in the spectra of both polymers. Two additional shoulders were observed at 1786 cm^{-1} and 1852 cm^{-1} in the modified PBS spectrum. These features are characteristic of anhydride carboxyl groups and similar results have been reported previously.[25] The shoulders represent free acids in the modified polymer and, therefore, denote the grafting of MA onto PBS.

The peak assigned to the O—H stretching vibration in the range of 3200–3700 cm^{-1} was more intense in the PBS/CSF (10 wt %) composite, as shown in Figure 1C, which is due to contributions from the —OH group of the CSF (Figure 1E).[26] The FTIR spectrum of the PBS-*g*-MA/TCSF (10 wt %) composite shown in Figure 1D had three peaks, one at 800–850 cm^{-1}, one at 1000–1150 cm^{-1}, and one at 1737 cm^{-1}, which were not present in the FTIR spectrum of the PBS/CSF (10 wt %) composite. These peaks were assigned to asymmetric stretching modes of Si—O—Si and/or Si—O—C bonds and the ester carbonyl stretching vibration of the PBS-*g*-MA/TCSF (10 wt %) composite, respectively.[27,28] These data suggest the formation of branched and crosslinked macromolecules in the PBS-*g*-MA/

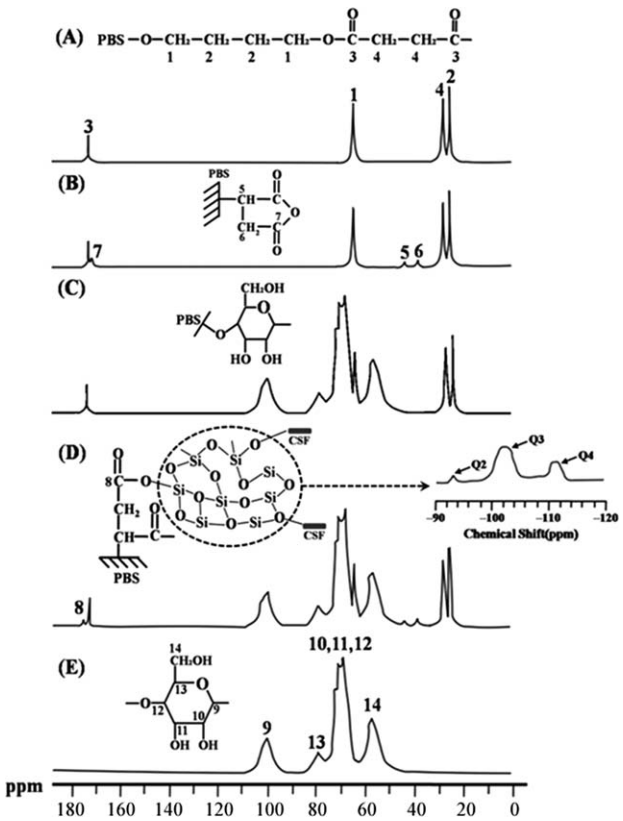

Figure 2. Solid-state ^{13}C NMR spectra. (A) PBS, where the numbered peaks are as follows: 1: $\delta = 64.3$ ppm; 2: $\delta = 25.1$ ppm; 3: $\delta = 172.5$ ppm; and 4: $\delta = 28.8$ ppm. (B) PBS-*g*-MA, where the numbered peaks are as follows: 5: $\delta = 42.3$ ppm, 6: $\delta = 35.9$ ppm, and 7: —C═O $\delta = 170.1$ ppm. (C) PBS/CSF (10 wt %), (D) PBS-*g*-MA/TCSF (10 wt %), and (E) CSF.

TCSF composite by covalent bonding of the anhydride carboxyl groups in PBS-*g*-MA with the hydroxyl groups of TCSF.

Solid-state ^{13}C NMR spectra of PBS and PBS-*g*-MA are shown in Figure 2(A,B), respectively. There were four peaks corresponding to carbon atoms in the unmodified PBS, which occurred at $\delta = 25.1$ ppm, $\delta = 28.8$ ppm, $\delta = 64.3$ ppm, and $\delta = 172.5$ ppm.[29] The ^{13}C NMR spectrum of PBS-*g*-MA showed additional peaks at $\delta = 42.3$ ppm, $\delta = 35.9$ ppm, and $\delta = 170.1$ ppm, which suggest that the MA was covalently grafted onto the PBS.

Solid-state ^{13}C NMR spectra of PBS/CSF (10 wt %), PBS-*g*-MA/TCSF (10 wt %), and CSF are shown in Figure 2(C–E), respectively. Relative to the unmodified PBS/CSF, additional peaks at $\delta = 35.9$ ppm and $\delta = 42.3$ ppm were observed in the spectra of composites containing PBS-*g*-MA/TCSF. Similar features have been reported previously,[30] indicating grafting of MA onto PBS. However, the peak at $\delta = 170.1$ ppm, which is attributed to C═O and is typical for MA grafted onto PBS, was absent in the solid-state spectrum of PBS-*g*-MA/TCSF (10 wt %).

The ^{13}C solid-state NMR and ^{29}Si solid-state NMR spectra of PBS/CSF (10 wt %) shown in Figure 2C also exhibited peaks not observed for neat PBS, which corresponded to the cross-linking agent in the TCSF. These are assigned as follows. Q_2: $\delta = -91$ to -93 ppm; Q_3: $\delta = -97$ to -101 ppm; and Q_4; $\delta = -110$ to -112 ppm.[31] ^{13}C solid-state NMR peaks originating from the reaction between MA in PBS-*g*-MA and —OH in TCSF were found at $\delta = 176.3$ ppm (see the peak numbered 13 in Figure 2D). These data, combined with the presence of the FTIR peaks at 1737 cm^{-1}, provide evidence of ester group formation due to the condensation of PBS-*g*-MA with TCSF. The formation of ester groups significantly affected the mechanical and biodegradation properties of PBS-*g*-MA/TCSF, which is discussed in greater detail in the following sections.

Morphology and Mechanical Properties

In most composite materials, effective wetting and uniform dispersion of all the components in a given matrix as well as strong interfacial adhesion between the phases are required to obtain a composite with satisfactory mechanical properties. Here, CSF or TCSF may be considered as a dispersed phase within a PBS or PBS-*g*-MA matrix. We used SEM images to evaluate the composite morphology and examine tensile fracture surfaces of PBS/CSF (10 wt %) and PBS-*g*-MA/TCSF (10 wt %) samples. The SEM image of PBS/CSF (10 wt %) shown in Figure 3A reveals that the CSF in this composite was evenly dispersed throughout the matrix. Poor adhesion occurred due to the formation of hydrogen bonds between the CSF, as well as the difference in the hydrophilicity between PBS and CSF. Poor wetting in these composites was also noted (see Figure 3A), which is attributed to the large difference in surface energies between the CSF and PBS matrix.[32] The SEM image of PBS-*g*-MA/TCSF (10 wt %) shown in Figure 3B reveals more uniform adhesion and better wetting of TCSF in the PHA-*g*-MA matrix, which is indicated by the complete coverage of PBS-*g*-MA on the TCSF and the removal of both materials when a TCSF fiber was pulled from the bulk. This improved interfacial adhesion is

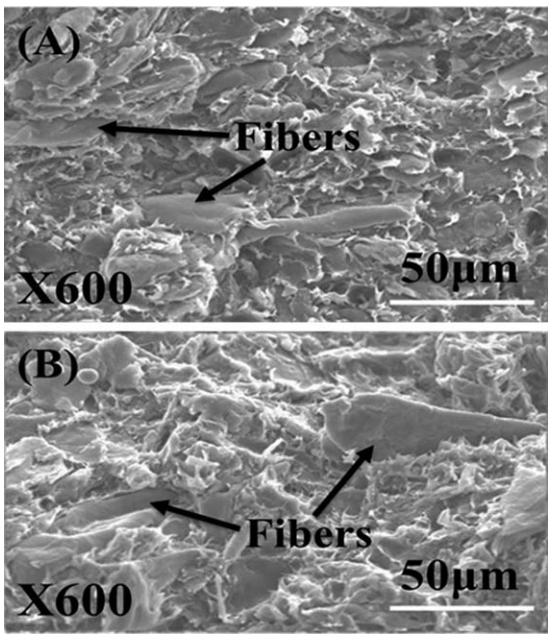

Figure 3. SEM images of the distribution and adhesion of fibers in (A) PBS/CSF (10 wt %) and (B) PBS-*g*-MA/TCSF (10 wt %) composites.

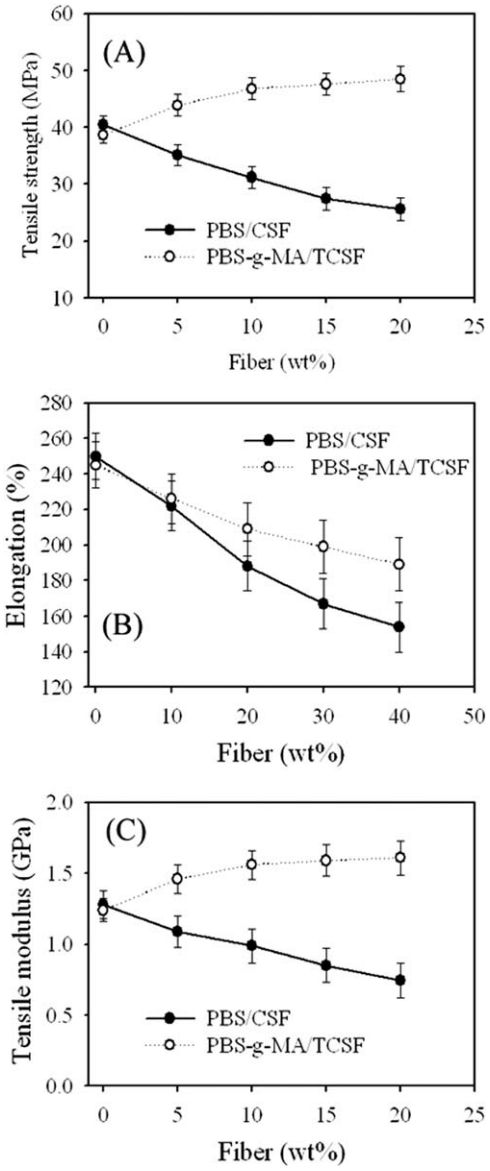

Figure 4. (A) The tensile strength at failure, (B) the elongation at failure, and (C) the tensile modulus for the PBS/CSF and PBS-*g*-MA/TCSF composites as a function of the CSF content.

attributed to the similar hydrophilicity of the two components, which allowed the formation of branched and crosslinked macromolecules and prevented hydrogen bonding between the TCSF fibers.

Figure 4 shows the tensile strength, tensile modulus, and elongation at failure as a function of the CSF or TCSF content for both the PBS/CSF and PBS-*g*-MA/TCSF composites. The tensile strength, tensile modulus, and elongation at failure of PBS-*g*-MA were all lower than those of PBS [see Figure 4(A–C)]. As shown in Figure 4(A,C), the tensile strength and tensile modulus at failure of the PBS/CSF composites decreased with increasing CSF content. This is attributed to poor dispersion of the CSF in the PBS matrix. However, the PBS-*g*-MA/TCSF composites exhibited an increase in the tensile strength and tensile modulus at failure with increasing TCSF content, and these composites exhibited superior mechanical properties compared to pure PBS. Furthermore, this increase in the tensile strength and tensile modulus at failure was observed for PBS-*g*-MA/TCSF composites saturated with TCSF contents above 10 wt %. This behavior is expected to result from enhanced dispersion of TCSF in the PBS-*g*-MA matrix resulting from the formation of branched or crosslinked macromolecules.

The data shown in Figure 4B reveal less elongation at failure for the PBS/CSF composites compared with that of the PBS-*g*-MA/

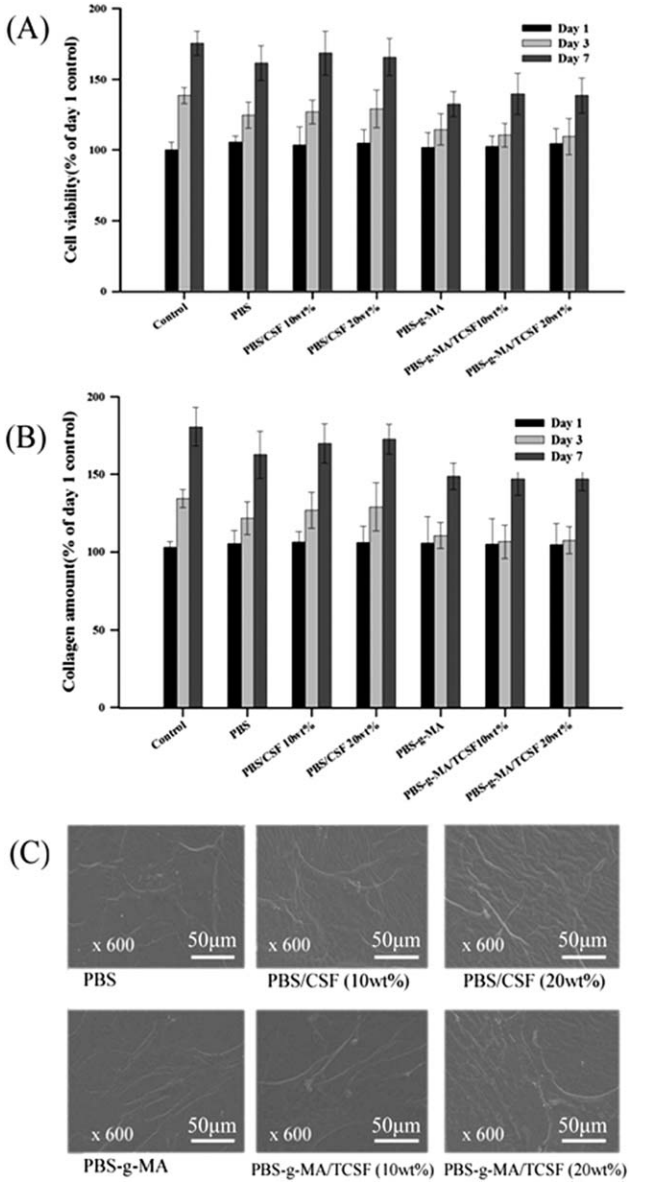

Figure 5. (A) Cell proliferation of normal human foreskin FBs seeded on the different composite membranes. The cell proliferation rate was quantified using an MTT assay over a period of 7 days. (B) The amount of collagen produced and secreted from human foreskin FBs seeded on the membranes over a period of 7 days. Sirius Red dye was used to quantify the amount of collagen. (C) SEM micrographs of human foreskin FBs and the collagen on the PBS, PBS-*g*-MA, PBS/CSF, and PBS-*g*-MA/TCSF membranes after 7 days of culture.

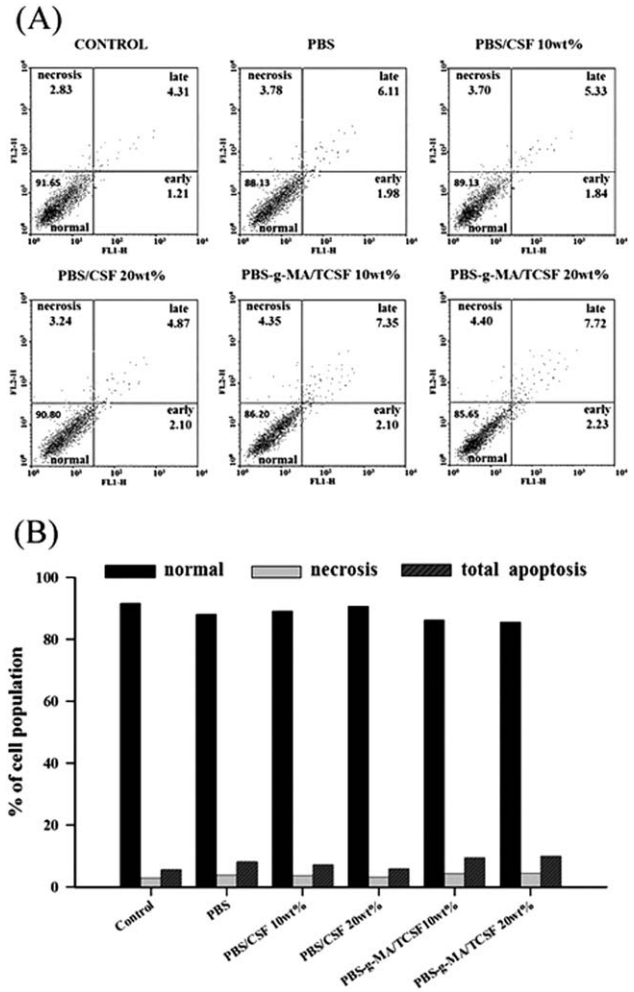

Figure 6. (A) The horizontal coordinates (FL1-H) represent cells stained by the Annexin V-FITC, and the vertical coordinates (FL2-H) represent the cells stained by PI. (B) These histograms represent the percentage of cell population in different phases.

TCSF composites. In PBS/CSF, the CSF tended to cover the matrix unevenly, illustrating the poor compatibility between the two phases. In the PBS-*g*-MA/TCSF composites, as shown in Figure 4C, the elongation at failure also decreased with increasing TCSF content, although the PBS-*g*-MA/TCSF composites exhibited more elongation at failure than the PBS/CSF composites. The data shown in Figure 4 indicate that the grafting reaction in PBS-*g*-MA/TCSF composites improved the tensile strength and tensile modulus and reduced the elongation at failure compared with pure PBS and with the PBS/CSF composite.

Biocompatibility of PBS and Its Composites

Cell Proliferation. The biocompatibility of the composites was evaluated by measuring the cell growth rate of normal FBs seeded on the membranes, as shown in Figure 5A. The cell viability was examined using MTT assays. The growth of FB cells on different membranes was measured on days 1, 3, and 7 for the different composites. On seeding the membranes, the PBS/CSF series membranes showed similar cell viabilities to FBs seeded on the plate directly from day 1 to 7, which reveals that the membranes had good compatibility with the FBs. The cell viability did not exhibit an obvious trend as a function of the CSF content, and the results were similar at CSF contents of 5 and 15 wt % (data not shown). The cell viabilities on the PBS-*g*-MA membranes were slightly lower than on the plate on day 1. On day 7, however, the cell viabilities on the PBS-*g*-MA membranes were quite similar to the PBS/CSF composites and the plate. The cell viability on the PBS-*g*-MA membranes was slightly lower than on the PBS/CSF membranes, which suggests a slight cytotoxic effect of the MA.

Amount of Collagen. Sirius Red dye was used to stain the collagen secreted by the dermal FBs on the well or on the membranes. Figure 5B shows the collagen production on the different membranes. This was similar at day 1. At days 3 and 7, collagen production on the PBS/CSF composites was higher than on the control plate. The rate of collagen production increased with the CSF content for the PBS/CSF composites. The rate of collagen production did not appear to depend on the CSF content in the PBS-*g*-MA composites, which showed a lower rate of collagen production than the PBS composites. At day 7, the collagen production on the PBS series membranes showed an obvious increase, which suggests that PBS series membranes stimulated collagen production and secretion by the FBs. After 7 days, the collagen secretion of FBs on the PBS-*g*-MA composites did not exhibit a noticeable enhancement, which may result from the cytotoxicity of MA.

Collagen is an important component for cell proliferation and tissue formation, both of which are dependent on FB production.[33] Collagen in the extracellular matrix imparts mechanical strength to the tissue, allowing it to maintain its shape.[34,35] Therefore, detecting the concentration of the collagen that is secreted is an important indicator of successful wound healing. As the PBS series membranes stimulated collagen secretion by the FB cells, these may be good biomaterials for tissue engineering on wound dressings. Figure 5C shows SEM images of collagen and FBs on the membranes after 7 days. Thread-like collagen formations can be seen on the membranes. These SEM data show the compacted fibril morphology of collagen. As the CSF content increased in the PBS/CSF composite, the SEM images show more secretion. This is consistent with the collagen quantification data shown in Figure 5B and suggests that these membranes may stimulate collagen production.

Cytotoxicity Assay. The nucleic acid stain PI and Annexin V-FITC were used for double-staining testing of HS68 cells, and flow cytometry was used for the analysis. When the cell undergoes apoptosis at an early age, the phosphatidyl serine inside the cell membrane translocates to the cell surface; therefore, the Annexin V-FITC can be used to stain cells. However, the cell membrane remains intact and the PI nucleic acid stain cannot penetrate the cell membrane. In a cell that undergoes necrosis, the phosphatidyl serine inside the cell membrane does not become exposed to the surface of the cell, the cell membrane ruptures, and the PI can stain the cell. Stained cells were quantified using flow cytometry analysis, and in this way we were able to determine the populations of normal cells, early- and late-stage apoptosis cells and necrotic cells.[36,37]

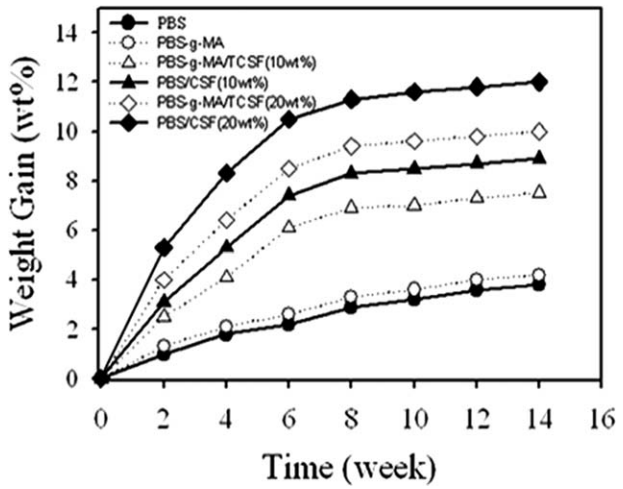

Figure 7. Percent weight gain from water absorption of the PBS/CSF and PBS-*g*-MA/TCSF composites as a function of time.

Figure 6 shows the populations of normal-, early-, and late-stage apoptosis, and necrotic HS68 cells on the PBS/CSF and PBS-*g*-MA/TCSF composites. The population of normal cells on the PBS/CSF composites was larger than on the PBS-*g*-MA/TCSF composites, because the addition of CSF enhances the biocompatibility of the material and is unlikely to lead to cell necrosis or apoptosis. In addition, the results show that the PBS-*g*-MA/TCSF composites resulted in more cell necrosis and apoptosis; this is attributed to the addition of MA, which results in slight cytotoxicity. The normal cell population in the PBS/CSF composites was 4–6% larger than on the PBS-*g*-MA/TCSF materials. No significant total (early and late) apoptosis or necrosis in the HS-68 cells was induced by PBS, PBS-*g*-MA, PBS/CSF, or PBS-*g*-MA/TCSF.

Water Absorption

Figure 7 shows the water absorption as a function of time. At a given fiber content, the PBS-*g*-MA/TCSF composites absorbed less water than the PBS/CSF composites. This water resistance of the PBS-*g*-MA/TCSF composites was moderate and is attributed to an increase in the hydrophobicity of TCSF due to interactions with the PBS-*g*-MA. For both PBS/CSF and PBS-*g*-MA/TCSF, the percent weight gain over the 14-week period increased with the CSF/TCSF content. Because the arrangement of polymer chains in these systems was supposedly random, these results were likely due to decreased chain mobility as the amount of fiber increased and to the hydrophilic nature of the fiber, which adhered weakly to the more hydrophobic PBS.

Biodegradation

Changes in the morphology of both the PBS/CSF and PBS-*g*-MA/TCSF composites were noted as a function of the time that they were buried in soil. SEM images taken after 6 and 12 weeks illustrated the extent of morphological change, as shown in Figure 8. The PBS/CSF composites [10 wt %; see Figure 8(E,F)] exhibited randomly distributed and larger pits than those in the PBS-*g*-MA/TCSF composites [10 wt %; see Figure 8(H,I)]. These analyses also indicate that biodegradation of the CSF

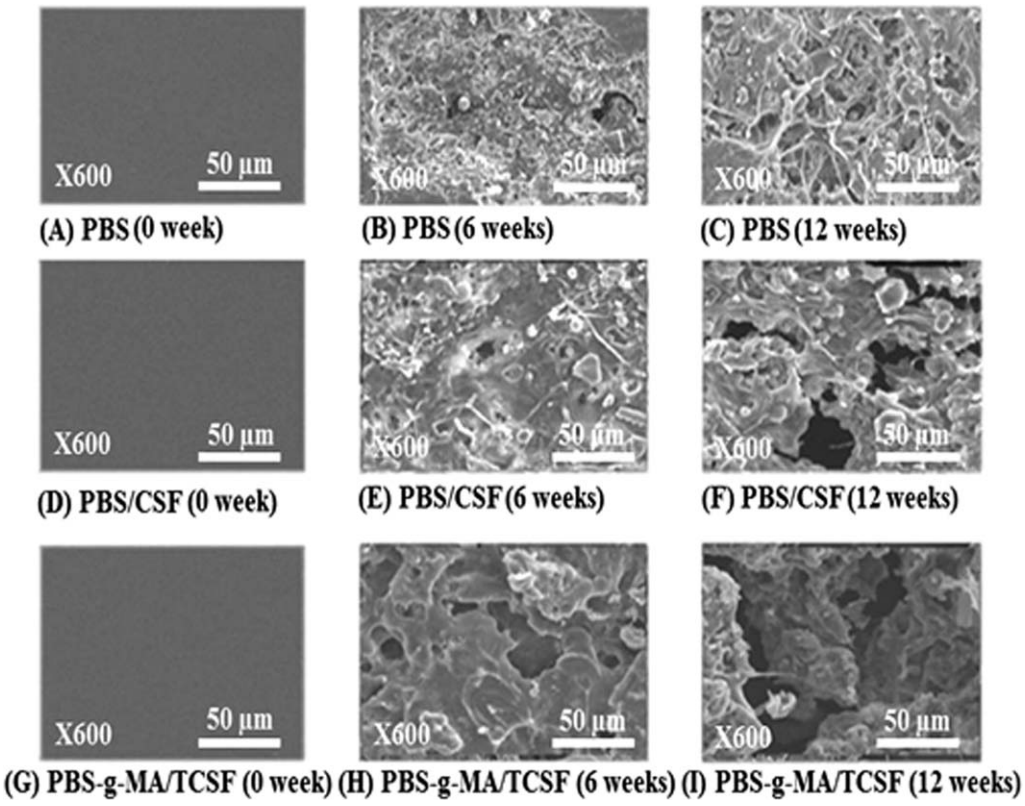

Figure 8. SEM images showing the morphology of (A–C) PBS, (D–F) PBS/CSF (10 wt %) and (G–I) PBS-*g*-MA/TCSF (10 wt %) films as a function of the incubation time in the soil.

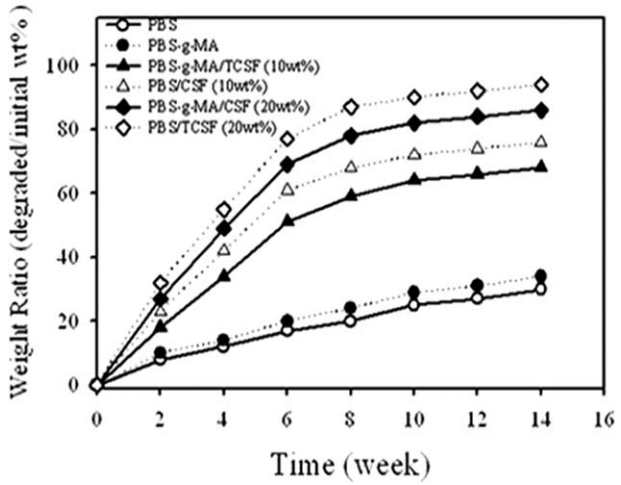

Figure 9. Weight loss of PBS, PBS-*g*-MA, PBS/CSF, and PBS-*g*-MA/TCSF as a function of the incubation time in the soil.

phase increased with time. After 6 weeks, disruption of the PBS matrix was obvious, as shown in Figure 8B. This degradation was confirmed by the weight loss of the PBS matrix as a function of time (see Figure 9), which reached nearly 27% after only 12 weeks. This weight loss is attributed to biodegradation. The SEM images in Figure 8 indicate that the PBS-*g*-MA/TCSF composites were more readily degraded than pure PBS. Moreover, at 6 and 12 weeks, larger pores were apparent in the PBS-*g*-MA/TCSF composites [see Figure 8(H,8I)], indicating a higher level of degradation. The rate of weight loss of the PBS-*g*-MA/TCSF composites was faster than that of PBS, exceeding 40% after 12 weeks. These results show that the addition of TCSF to the PBS-*g*-MA enhanced the biodegradability of the composite.

Figure 9 shows the percent weight change as a function of time for the PBS/CSF and PBS-*g*-MA/TCSF composites buried in the soil compost. For both the composites, the degree of weight loss increased with fiber content. Composites with 10 wt % of fibers degraded rapidly over the first 6 weeks, losing mass approximately equivalent to their fiber content, and then showed a more gradual decrease in weight over the next 6 weeks. PBS/CSF exhibited approximately 5–10 wt % more weight loss than PBS-*g*-MA/TCSF.

CONCLUSIONS

Composites of MA-modified PBS with crosslinked TCSF were studied. FTIR and NMR analyses revealed the formation of ester groups in the composites, formed by reactions between the hydroxyl groups of the TCSF and the anhydride carboxyl groups of PBS-*g*-MA. The morphology of the PBS-*g*-MA/TCSF composites was consistent, with good adhesion between the TCSF phase and the PBS-*g*-MA matrix. Mechanical tests showed that the improved adhesion between TCSF and PBS-*g*-MA enhanced the mechanical properties of the composites. Cell viability tests and apoptosis assay indicated that the PBS membranes showed good biocompatibility toward FB proliferation. Collagen secretion by FBs on the PBS-series composite samples demonstrates potential for the use of PBS/CSF membranes as scaffolds for tissue engineering. The water resistance of PBS-*g*-MA/TCSF was higher than that of PBS/CSF. When incubated in soil, the biodegradation rate of PBS-*g*-MA/TCSF was slower than that of PBS/CSF but still significantly higher than that of pure PBS. The rate of biodegradation increased with increasing fiber content.

ACKNOWLEDGMENTS

The author thanks the National Science Council (Taipei City, Taiwan, ROC) for financial support (NSC-102-2621-M-244-001).

REFERENCES

1. Azadeh, S.; Murugan R.; Imen, E. H.; Serge, O.; K. Ali. *Acta Biomater.* **2011**, *7*, 1441.
2. Holzapfel, B. M.; Reichert, J. C.; Schantz, J. T.; Gbureck, U.; Rackwitz, L.; Nöth, U.; Jakob, F.; Rudert, M.; Groll, J.; Hutmacher, D. W. *Adv. Drug. Deliv. Rev.* **2013**, *65*, 581.
3. Burnouf, T.; Goubran, H. A.; Chen, T. O.; Ou, K. L.; Magdy, E.; Radosevic, M. *Blood Rev.* **2013**, *27*, 77.
4. Xiang, Y.; Wang, Y.; Luo, Y.; Zhang, B.; Xin, J.; Zheng, D. *Colloids Surf. B* **2011**, *85*, 248.
5. Kundu, B.; Rajkhowa, R.; Kundu, S. C.; Wang, X. *Adv. Drug. Deliv. Rev.* **2013**, *65*, 457.
6. Kim, G.; Rho, Y.; Park, S.; Kim, H.; Son, S.; Kim, H.; Kim, I. J.; Kim, J. R.; Kim, W. J.; Ree, M. *Biomaterials* **2010**, *31*, 3816.
7. Peter, M.; Binulal, N. S.; Soumya, S.; Nair, S. V.; Furuike, T.; Tamura, H.; Jayakumar, R. *Carbohydr. Polym.* **2010**, *79*, 284.
8. You, Z.; Cao, H.; Gao, J.; Shin, P. H.; Day, B. W.; Wang, Y. *Biomaterials* **2010**, *31*, 3129.
9. Nair, L. S.; Laurencin, C. T. *Prog. Polym. Sci.* **2007**, *32*, 762.
10. Ko, Y. G.; Ma, P. X. *J. Colloid Interface Sci.* **2009**, *330*, 77.
11. Lovell, C. S.; de Oca, H. M.; Farrar, D.; Ries, M. E.; Ward, I. M. *Polymer* **2010**, *51*, 2013.
12. Pan, P.; Inoue, Y. *Prog. Polym. Sci.* **2009**, *34*, 605.
13. Liang, J.; Zhou, L.; Tang, C. Y.; Tsui, C. P.; Li, F. *J. Polym. Test* **2012**, *31*, 149.
14. Weng, Y. X.; Jin, Y. J.; Meng, Q. Y.; Wang, L.; Zhang, M.; Wang, Y. Z. *Polym. Test* **2013**, *32*, 918.
15. Liu, L.; Yu, J.; Cheng, L.; Yang, X. *Polym. Degrad. Stab.* **2009**, *94*, 90.
16. Kim, H. S.; Kim, H. J.; Lee, J. W.; Choi, I. G. *Polym. Degrad. Stab.* **2006**, *91*, 1117.
17. Phua, Y. J.; Lau, N. S.; Sudesh, K.; Chowa, W. S.; Mohd Ishak, Z. A. *Polym. Degrad. Stab.* **2012**, *97*, 1345.
18. Zhao, Q.; Tao, J.; Yam, R. C. M.; Mok, A. C. K.; Li, R. K. Y.; Song, C. *Polym. Degrad. Stab.* **2008**, *93*, 1571.
19. Wong, K. J.; Zahi, S.; Low, K. O.; Lim, C. C. *Mater. Des.* **2010**, *31*, 4147.
20. Prasad, A. V.; Rao, K. M. *Mater. Des.* **2011**, *32*, 4658.
21. De Vasconcelos, M. C. B. M.; Bennett, R. N.; Rosa, A. S. E.; Ferreira-Cardoso, J. V. *J. Sci. Food Agric.* **2010**, *90*, 1578.
22. Hwang, S. W.; Lee, S. B.; Lee, C. K.; Lee, J. Y.; Shim, J. K.; Selke, S. E. M.; Soto-Valdez, H.; Matuana, L.; Rubino, M.; Auras, R. *Polym. Test* **2012**, *31*, 333.

23. Umare, S. S.; Chandure, A. S.; Pandey, R. A. *Polym. Degrad. Stab.* **2007**, *92*, 464.
24. Sahoo, S.; Misra, M.; Mohanty, A. K. *Compos Part A* **2011**, *42*, 1710.
25. Xiong, Z.; Li, C.; Ma, S.; Feng, J.; Yang, Y.; Zhang, R.; Zhu, J. *Carbohydr Polym* **2013**, *95*, 77.
26. Yao, Z.; Qi, J.; Wang, L. *J Food Sci* **2012**, *77*, C671.
27. Kim, H. S.; Lee, B. H.; Choi, S. W.; Kim, S.; Kim, H. *J. Compos Part A* **2007**, *38*, 1473.
28. Pothan, L. A.; Thomas, S.; Groeninckx, G. *Compos Part A* **2006**, *37*, 1260.
29. Kuwabara, K.; Gan, Z.; Nakamura, T.; Abe, H.; Doi, Y. *Biomacromolecules* **2002**, *3*, 1095.
30. Ranganathan, S.; Baker, W. E.; Russell, K. E.; Whitney, R. A. *J. Polym. Sci. Part A: Polym. Chem.* **1999**, *37*, 3817.
31. Wu, C. S.; Liao, H. T. *Des. Monomers Polym.* **2003**, *6*, 1.
32. Trana, L. Q. N.; Fuentesa, C. A.; Dupont-Gillain, C.; Van Vuure, A. W.; Verpoest, I. *Colloids Surf. A* **2011**, *377*, 251.
33. Nam, K.; Kimura, T.; Funamoto, S.;Kishida, A. *Acta Biomater.* **2010**, *6*, 409.
34. Sivakumar, L.; Agarwal, G. *Biomaterials* **2010**, *3*, 4802.
35. Grover, C. N.; Cameron, R. E.; Best, S. M. *J. Mech. Behav. Biomed. Mater.* **2012**, *10*, 62.
36. Veleirinho, B.; Coelho, D. S.; Dias, P. F.; Maraschin, M.; Ribeiro-do-Valle, R. M.; Lopes-da-Silva, J. A. *Int. J. Biol. Macromol.* **2012**, *51*, 343.
37. Bhattacharyya, S. S.; Paul, S.; De, A.; Das, D.; Samadder, A.; Boujedaini, N.; Khuda-Bukhsh, A. R. *Toxicol. Appl. Pharmacol.* **2011**, *253*, 270.